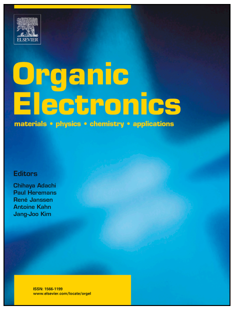

Rapid and green synthesis of complementary D-A small molecules for organic photovoltaics

Jérémie Grolleau, Frédéric Gohier, Magali Allain, Stéphanie Legoupy, Clément Cabanetos, Pierre Frère

PII: S1566-1199(16)30585-7
DOI: 10.1016/j.orgel.2016.12.046
Reference: ORGELE 3895

To appear in: *Organic Electronics*

Received Date: 16 October 2016
Revised Date: 19 December 2016
Accepted Date: 22 December 2016

Please cite this article as: J. Grolleau, F. Gohier, M. Allain, S. Legoupy, C. Cabanetos, P. Frère, Rapid and green synthesis of complementary D-A small molecules for organic photovoltaics, *Organic Electronics* (2017), doi: 10.1016/j.orgel.2016.12.046.

Rapid and green synthesis of complementary D-A small molecules for organic photovoltaics

Jérémie Grolleau, Frédéric Gohier, Magali Allain, Stéphanie Legoupy, Clément Cabanetos and Pierre Frère**

University of Angers, MOLTECH-Anjou UMR CNRS 6200, SCL group, 2 boulevard Lavoisier, 49045 Angers cedex

*Corresponding authors. Fax +33 2 41 73 54 05

E-mail: pierre.frere@univ-angers.fr, stephanie.legoupy@univ-angers.fr

KEYWORDS. Organic Photovoltaics, Direct Arylation, Knoevenagel reactions, Green chemistry.

ABSTRACT. Two push-pull molecules with close molecular structures have been synthesized through two green steps, direct heteroarylation and Knoevenagel condensation. The electronic properties and the basic bilayer heterojunction solar cells demonstrate that the two molecules are complementary in term of light absorption. Thus solar cells using a blend of the two molecules present higher power conversion efficiencies, reaching 3%, than the cells made from each compound alone.

Introduction

Organic photovoltaics (OPV) represent a promising source of low-cost electricity production with expected lower environmental impact than silicon based solar cells.[1, 2] Up until recently, most of research efforts on organic solar cells (OSCs) has been devoted/focusing on the fabrication of bulk heterojunction (BHJ) organic solar cells, prepared from a blend of a p-type conjugated materials, polymers or small molecules, and a n-type soluble fullerene derivative.[3, 4] Optimization of donor materials from the chemical point of view, *ie*, by studying structure/property relationships, has led to photovoltaic devices with high performances. However, these improvements are often associated with increased complexity of both the device and the structure of the donor materials, hence inducing longer tedious synthetic procedures.[5] The design of donor materials based on the donor – acceptor (D-A) concept consisting of alternating an electron rich block and an electron deficient unit in the π-conjugated backbone to tune the electronic properties, has allowed to reach the highest power conversion efficiencies (PCE) above 10%.[6-8] Nevertheless, considering the time-consuming of multistep synthesis, often involving organometallic coupling reactions that require a high degree of purification with manipulation of large amount of solvents,[9] it still falls far short of the prerequisites to assume the green and low-cost criteria for the conception of most conjugated materials.

Recent articles focused on the necessity of developing cheaper and cleaner routes for active materials production for future industrial development of organic photovoltaic cells.[9-12] Cheaper route towards organic semiconductors can be achieved by a simplification of the conjugated structures. Recently, several groups have reported new small push-pull molecules with chemical structures based on arylamine donor moiety, such as triphenylamine, linked to small acceptor unit through a more or less short conjugated spacer.[7, 13-22] Depending on the latter, the relative simplicity of the molecular architectures allows an access to the final compounds within two or maximum four steps with global yields of *ca* 65 %. Additionally, simple modifications of the donor and/or acceptor block induce a fine tuning of their electronic and photovoltaic properties affording both high open circuit voltage (V_{OC}) and short circuit current density (J_{SC}).

In our continuous effort to design simple and easily accessible molecular architectures for developing cleaner conjugated materials for OSCs,[23, 24] we have focused our efforts on the green and rapid synthesis of the push-pull molecules **DA1** [17] and **DA2**. Regarding **DA2**, the small structural modification of **DA1** by grafting a cyano group on the thiophene connector, has been designed to strengthen the acceptor character of the push-pull molecule and thus to decrease the band gap of the corresponding material.

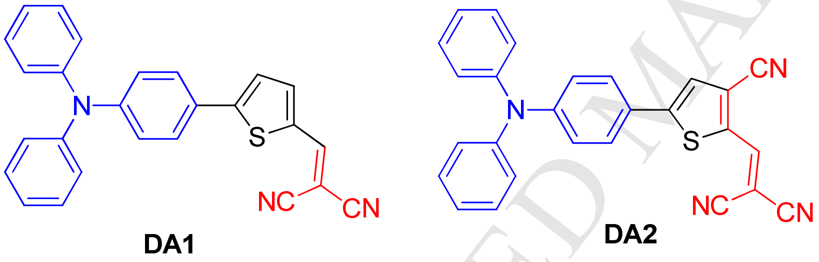

Figure 1. Structure of **DA1** and **DA2**

Experimental

Synthesis

4-bromo-*N*,*N*-diphenylaniline and 2-formylthiophene are commercially available. 2-formyl-3-cyanothiophene 2 was obtained by the regioselective deprotonation of 3-cyanothiophene followed by treatment with DMF.

<u>2-formyl-3-cyanothiophene **2**</u>

Under an argon atmosphere, solution of *n*-BuLi 2.5M in hexane (9 mL, 22.50 mmol) was added dropwise to a solution of diisoproylamine (3.6 mL, 25.69 mmol) in dry THF (20 mL) cooled to -78°C. After stirring for 20 min, lithium diisopropylamine was added at -78°C to a solution of thiophene-3-carbonitrile (2.1 mL, 23.09 mmol) in anhydrous THF (40 mL), after 30 min was added dimethylformamide (2.8 mL, 36.16 mmol). The mixture was slowly warmed to room temperature and stirred for 16h. The organic layer was washed with water and solution of HCl (2 M), dried over $MgSO_4$ and the solvent was evaporated. The crude was purified by chromatography over silica gel (Pentane/AcOEt: 95/5) to give a white powder (1.39 g, yield: 44%).

MP: 84-86°C
IR: υ = 2233 cm^{-1} (C≡N), 1672 cm^{-1} (C=O).
NMR ^1H ($CDCl_3$): 10.14 (d, 1H, *J*=1.2 Hz), 7.84 (dd, 1 H, *J*=1.2 Hz, *J*=5.0 Hz), 7.44 (d, 1H, *J*=5.0 Hz).
NMR ^{13}C ($CDCl_3$): 180.5, 149.2, 135.0, 131.0, 116.5, 112.8.
HRMS (EI) calcd for C_6H_3NOS [M^+]: 136.9935, found: 136.9932.

Direct coupling arylation

To a solution of 4-bromo-*N*,*N*-diphenylaniline (709 mg, 2.19 mmol), potassium carbonate (458 mg, 3.32 mmol, 1.5 eq), palladium acetate (30.80 mg, 6%mol), pivalic acid (70 mg, 0.69 mmol, 30%mol) and tricyclohexylphosphine tetrafluoroborate (104 mg, 0.28 mmol, 12%mol) in toluene (30 mL) degassed with argon during 20 min was added 2 formylthiophene (500 mg, 4.45 mmol) or 2-formylthiophene-3-carbonitrile (600 mg, 4.38 mmol). The mixture was stirred at 100°C during 16h, cooled and poured into water. The organic layer was extracted with ethyl acetate (2 times), dried over $MgSO_4$, filtered, and solvent was removed. The residue was purified by chromatography on silica gel (Hexane / AcOEt: 60/40).

5-(4-(diphenylamino)phenyl)thiophene-2-carbaldehyde: **3**

715 mg, 92% yield. Red solid.

MP: 88-90 °C[17, 25]

NMR ^{1}H (CDCl$_3$): 9.85 (s, 1H); 7.71 (d, 1H, *J*=4.0Hz); 7.52 (d, 2H, *J*=8.8Hz); 7.34-7.26 (m, 5H); 7.17-7.05 (m, 8H).

NMR ^{13}C (CDCl$_3$): 182.8, 154.8, 149.4, 147.2, 141.6, 137.9, 129.7, 127.5, 126.4, 125.4, 124.1, 123.1, 122.6.

HRMS (FAB) calcd for $C_{23}H_{17}NOS$ [M$^+$]: 355.1031, found: 355.1028

5-(4-(diphenylamino)phenyl)-2-formylthiophene-3-carbonitrile**: 4**

773 mg, 93 % yield. Red solid.

MP: 159-161°C.

IR: υ = 2230 cm^{-1} (C≡N), υ = 1658 cm^{-1} (C=O).

NMR ^{1}H (CDCl$_3$): 10.07 (s, 1H), 7.48-7.43 (m, 3H), 7.35-7.30 (m, 4H), 7.16-7.11 (m, 6H), 7.07-7.04 (m, 2H).

NMR ^{13}C (CDCl$_3$): 180.3, 154.8, 150.3, 146.7, 145.4, 129.8, 127.5, 125.7, 124.6, 124.5, 123.7, 121.7, 117.5, 113.0.

HRMS (FAB) calcd for $C_{24}H_{16}N_2OS$ [M$^+$]: 380.0983, found: 380.0987.

Knoevenagel reaction by ball milling process

General procedure. A mixture of (diphenylamino)phenyl)thiophene-carbaldehyde **3** or **4** (1 mmol) and malononitrile (1 mmol) with solid potassium acetate (10 % mol) were ball-milled at room temperature during 30 min. with frequency of 30 Hz. The red or purple solid was recovered then washed with a mixture of EtOH – Pentane (20 mL, 6/4). The solid was purified by flash chromatography on silica gel (Hexane/AcOEt: 8/2) to give a red-brown or a purple powder.

2-((5-(4-(diphenylamino)phenyl)thiophen-2-yl)methylene)malononitrile: **DA1**

383 mg, 95% yield. Red brown solid.

MP = 185-188°C

NMR ^{1}H (CDCl$_3$): 7.74 (s, 1H); 7.68 (d, 1H, *J*=4.0 Hz); 7.53 (d, 2H, *J*=8.8 Hz); 7.34-7.29 (m, 5H); 7.16-7.10 (m, 6H); 7.05 (d, 2H, *J*=8.8Hz).

NMR ^{13}C (CDCl$_3$): 157.3, 150.4, 150.1, 146.7, 140.5, 133.2, 129.7, 127.7, 125.6, 125.0, 124.5, 123.4, 121.8, 114.7, 113.8, 75.1.

HRMS (FAB) calcd for $C_{26}H_{17}N_3S$ [M^+]: 403.1143, found: 403.1137.

Elemental Anal. calcd for $C_{26}H_{17}N_3S$: C, 77.39; H, 4.25; N, 10.41 found: C, 77.13; H, 4.26; N, 10.44.

2-((3-cyano-5-(4-(diphenylamino)phenyl)thiophen-2-yl)methylene)malononitrile: **DA2**

406 mg, 95% yield. Purple solid.
MP: 215-217°C.

IR: υ = 2226 cm^{-1} (C≡N).

NMR ^1H ($CDCl_3$): 7.99 (s, 1H), 7.51-7.48 (m, 3H), 7.37-7.31 (m, 4H), 7.18-7.14 (m, 6H), 7.05-7.03 (m, 2H).

NMR ^{13}C ($CDCl_3$): 156.4, 151.1, 146.5, 146.3, 137.5, 129.9, 127.9, 126.0, 125.1, 124.0, 122.7, 121.1, 120.5, 113.5, 112.8, 79.9.

HRMS (FAB) calcd for $C_{27}H_{16}N_4S$ [M^+]: 428.1096, found: 428.1087.

Elemental Anal. calcd for $C_{27}H_{16}N_4S$: C, 75.68; H, 3.76; N, 13.07; found: C, 75.70; H, 3.76; N, 12.99.

Crystal Data and Structure Refinement

Single crystals of **DA2** suitable for X-ray diffraction analysis were obtained by slow evaporation of a mixture of ethanol- chloroform solution. The compound crystallizes in the monoclinic C2/c space group. X-ray single-crystal diffraction data were collected at 293 K on a BRUKER KappaCCD diffractometer, equipped with a graphite monochromator utilizing Mo Kα radiation (λ = 0.71073 Å). The structure was solved by direct methods and refined on F2 by the full-matrix least-squares method using the SHELX97 package. All non-H atoms were refined anisotropically, and absorption was corrected by the SADABS program. The H atoms were included in the calculation without refinement.

Crystallographic Data for DA2.

$C_{27}H_{16}N_4S$, M = 428.5, red plate, 0.30 × 0.25 × 0.06 mm^3, monoclinic, space group C2/c, a = 31.315(3) Å, b = 8.1924(5) Å, c =17.832(2) Å, α = 90°, β = 103.555(9)°, γ = 90°, V

=4447.3(7) Å^3, Z =8, ρ_{calc} =1.280 g/cm^3, μ(Mo Kα) = 0.167 mm^{-1}, F(000) = 1776, θmin = 3.20°, θmax = 27.49°, 23142 reflections collected, 5068 unique (Rint = 0.0535), parameters/restraints = 289/0, R1 = 0.0603 and wR2 = 0.0975 using 2951 reflections with $I > 2\sigma(I)$, R1 = 0.1293 and wR2 = 0.1188 using all data, GOF = 1.057, $-0.248 < \Delta\rho < 0.208$ e.Å^{-3}. CCDC- 1486170.

Preparation of the solar cells

Indium-tin oxide coated glass slides of 24×25×1.1 mm with a sheet resistance of RS = 10 Ω/sq were purchased from VisionTek Systems Ltd. The substrates were scrubbed using dishwashing soap before being cleaned by a series of ultrasonic treatments for 15 min in distilled water, acetone, and isopropanol. Once dried under a steam of nitrogen, a UV-ozone plasma treatment (UV/Ozone ProCleaner Plus, Bioforce Nanosciences) was performed for 15 min. A filtered aqueous solution of poly(3,4-ethylenedioxy-thiophene)-poly(styrenesulfonate) (PEDOT:PSS; Clevios P VP. AI 4083) through a 0.45 μm RC membrane (Millex®) was spun-cast onto the patterned ITO surface at 5000 rpm for 40 s before being baked at 115°C for 15 min. The best devices were obtained with films spun-cast from chloroform solutions at 6000 rpm for **DA1**, **DA2** and Blend containing 10 mg/mL of material(s). Finally, OSCs were completed by the successive thermal deposition of C_{60} (30 nm) and aluminum (80 nm) at a pressure of 10^{-6} Torr through a shadow mask defining two cells of 27 mm^2 each. J vs V curves were recorded in the dark and under illumination using a Keithley 236 source-measure unit and a home-made acquisition program. The light source is an AM1.5 Solar Constant 575 PV simulator (Steuernagel Lichttecknik, equipped with a metal halogen lamp). The light intensity was measured by a broad-band power meter (13PEM001, Melles Griot). EQE was recorded under ambient atmosphere using a halogen lamp (Osram) with an Action Spectra Pro 150 monochromator, a lock-in amplifier (Perkin-Elmer 7225) and a S2281 photodiode (Hamamatsu).

Space charge limited current (SCLC) measurements

A solution of molecular donor (10 mg/mL) in chloroform was spun cast at 1500 rpm on the above described PEDOT: PSS substrates to provide organic layers of ca 80 nm. Gold cathodes (150 nm) were thermally evaporated under a vacuum of 10^{-6} Torr, through a shadow mask defining actives area of 12.60 mm², 3.10 mm² and 0.78 mm² per substrates. Hole mobilities μ_h were evaluated using the Mott-Gurney law, ie, $J_{SCLC} = (9/8)\varepsilon_0\varepsilon_r\ \mu_h(V^2/d^3)$ where ε_0 is the permittivity of free space, ε_r is the static dielectric constant of the medium ($\varepsilon_r = 3$), V is the voltage applied and d the thickness of the active layer.[26]

Results and discussion

As depicted in scheme 1, the synthesis of the titled derivatives has been carried out in two green steps. First, the commercially available 4-bromo-triphenylamine (TPA-Br) was engaged in a direct arylation reaction with the aldehydes **1** or **2** affording the extended derivatives **3** and **4**. The latter were then engaged in a Knovenagel condensation with malononitrile yielding the titled donors **DA1** and **DA2**. In addition, it is worth noting that greener procedures have been studied for these two steps.

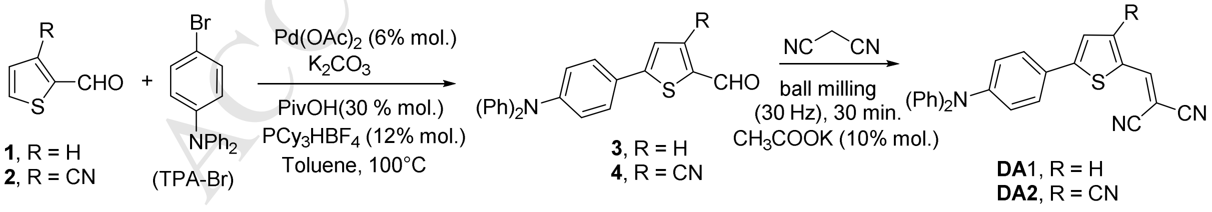

Scheme 1: Green synthesis of compounds **DA1** and **DA2**.

Regarding the direct arylation coupling, several procedures have been examined. All the results are summarized in Table 1. The procedure described by Fagnou et al.[27] has been first applied (entries 1 and 2) by using 1 equivalent TPA-Br and 2 equivalents of thiophene aldehyde (**1** or **2**), K_2CO_3 (3 equiv.), $Pd(OAc)_2$ (6 mol %), pivalic acid (PivOH, 30 mol %), phosphine derivative PCy_3HBF_4 (10-12 mol %) at 100°C in toluene for 16 h. Compounds **3** and **4** were isolated in 92 and 93 % yield respectively. As the excesses of aldehyde reactants 1 and 2 were not recurved, attempts were also performed by using a stoichiometric amount of reactants (entries 3 and 4) to give an acceptable 72 % yield for **3**, but a very low yield of ca 8% for **4**.

Table 1. Direct arylation between thiophene aldehydes **1** and **2** with TPA-Br using various condition

Entry	Thiophene aldehyde	TPA-Br Amount equiv	Additives	Yield[a] (%)
1	**1**	0.5	PCy_3HBF_4 (12%) PivOH (30%)	92
2	**2**	0.5	PCy_3HBF_4 (12%) PivOH (30%)	93
3	**1**	1.0	PCy_3HBF_4 (12%) PivOH (30%)	72
4	**2**	1.0	PCy_3HBF_4 (12%) PivOH (30%)	8

[a] Yields are isolated,

The Knoevenagel condensation between the corresponding aldehydes (**3** and **4)** and malononitrile were then carried out, affording **DA1** and **DA2** in simplified green procedures. By contrast with the usual method using chloroform in presence of piperidine or Et_3N,[17, 21, 28, 29] condensations without solvent by ball-milling technique have been performed.[30, 31] The reactions proceeded with quantitative yields after 30 min of stirring at room temperature of a blend of aldehyde (**3** or **4**), malononitrile (1 equivalent) and potassium acetate (10 mol %). Highly pure materials were isolated in 95 % yield after a flash chromatography on silica gel. The condensation can be also performed by reflux of ethanol solution during 16h with an excess of malononitrile (2 equivalents) to give **DA1** and **DA2** in 90% yields. At room temperature in ethanol in presence of catalytic amount of tBuONa, the yields for obtaining the two compounds decrease to 70 %. Finally, the ball- milling technique gives the best results in terms of efficiency and rapidity while handling a minimum of solvent.

Thus the two compounds were prepared in two steps with a global yield of ca 85%. To evaluate the environmental impact of these new synthesis of **DA1**, the amount of waste produced per gram (E factor)[32] has been calculated and compared with the conventional synthetic routes using organometallic coupling reactions (Stille and Suzuki cross couplings) for the first step. For the calculation of the E factor, the criteria defined by Osedach et al. have been used (see Figure S1-S4 in supplementary materials).[12] The access to **DA1** from TPA-Br and the commercially available thiophene carbaldehyde **1** via the direct C-H arylation gives an E factor of 903. The greener method of this procedures, including the Knoevenagel reaction in ball mills, is clearly demonstrated by comparing with the E factors obtained when Suzuki coupling reaction was used (E = 1636).[25] In this procedure, if the coupling reaction did not produce more wastes than for the direct-arylation way, the synthesis of the boronic derivative in two steps from thiophene carbaldehyde[33] participates for 30 % in the E factor. The synthesis of **DA1** via Stille coupling reaction[17] leads to an even higher E factor (E = 3445). The preparation and the use of the stannyl derivative of thiophene participates for 50% in the E factor. The step of formylation by Vilsmeir-Haack reaction also generates a large amount of wastes.

Finally, the synthesis of compound **DA2**, results in an E factor of 1572 including the preparation of the 3-cyano-2-formylthiophene **2** from the commercially available 3-cyanothiophene.

The crystallographic structures of **DA2** single crystals, obtained from a slow evaporation of ethanol-chloroform solutions, have been analysed by X-Ray diffraction. The latter crystallizes in the monoclinic C1 2/c1 space group. It is important to note that the conformation adopted by **DA2** (Figure 2a) is similar to that obtained for **DA1**.[17, 18] The dicyanovinyl (DCV) moiety is in the plane defined by the 3-cyanothiophene unit and adopts a *cis* conformation relative to the sulfur atom. The two outermost phenyl rings of the TPA unit are out of the plane defined by the thiophene and DCV systems while the torsional angle between the connected phenyl and thiophene cycles is of 19.1°. The structure is characterized by two axes of stacking which are quasi perpendiculars (Figure 2b). In each column, the stacking of the molecules is done so that each molecule presents several short interatomic distances less than 3.6 Å with three other molecules as shown by dotted blue lines in Figure 2c.

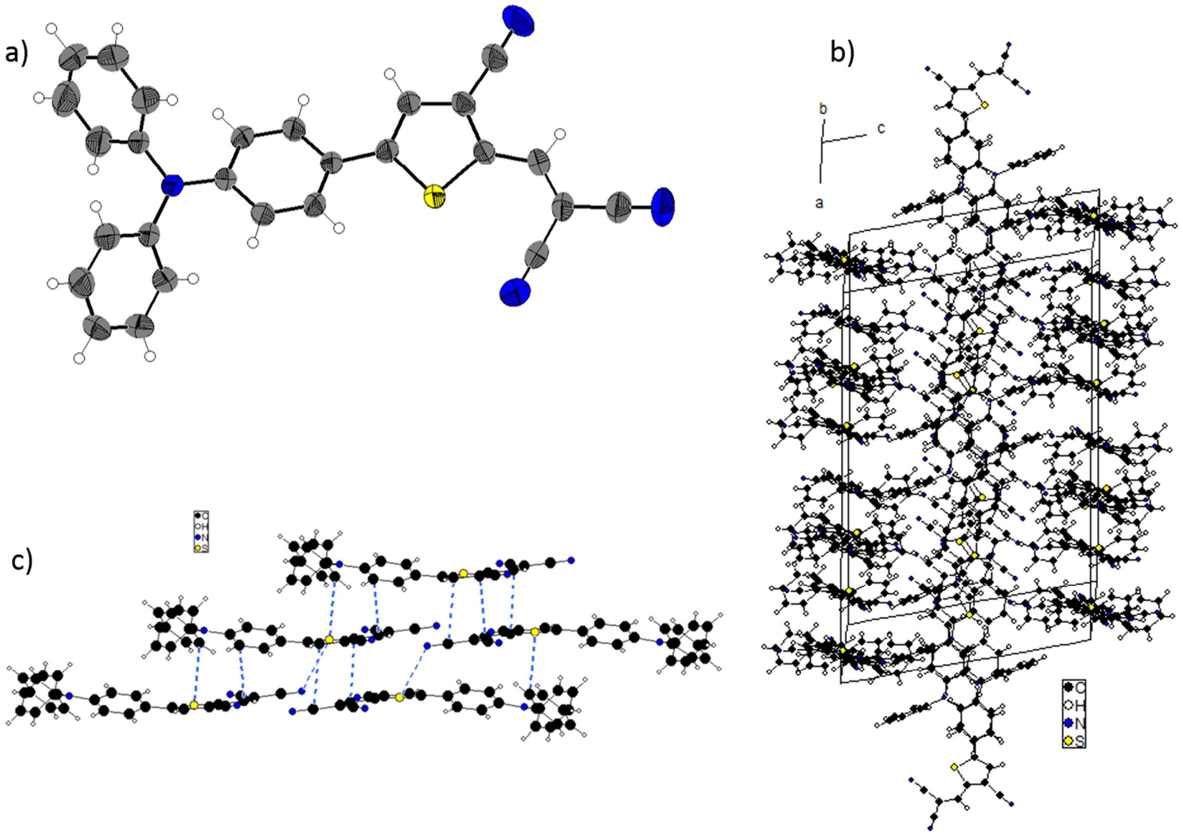

Figure 2: Single-crystal X-ray structure of **DA2**.

The influence of the cyano group borne by the thiophene connector on the electronic properties has been evaluated by theoretical calculations performed at the ab initio density functional level with the Gaussian 09 package. Becke's three-parameter gradient-corrected functional (B3LYP) with a polarized 6-31G (d,p) basis was used for full geometry. The contours of the HOMO and LUMO orbitals and a schematic evolution of their levels are illustrated in Figure 3. The optimized structures of the two compounds are almost identical and, they present planar structures of the conjugated backbones and a torsion of the outermost phenyl units of TPA. The HOMO are mainly allocated on the TPA – Thiophene units and the carbon atoms of thiophene internal at TPA whereas LUMO are localized on the thiophene - dicyanovinyl moieties as well as the extra cyano group borne by **DA2**. Such contribution of this cyano group led to a strong stabilisation of the LUMO level and a moderate stabilisation of the HOMO level for **DA2** compared to **DA1**, resulting in a reduction of the band gap of ca 0.3 eV for **DA2**. Thus, both a red shift of the absorption band and a positive shift of the reduction potential are expected for **DA2** compared to **DA1**.

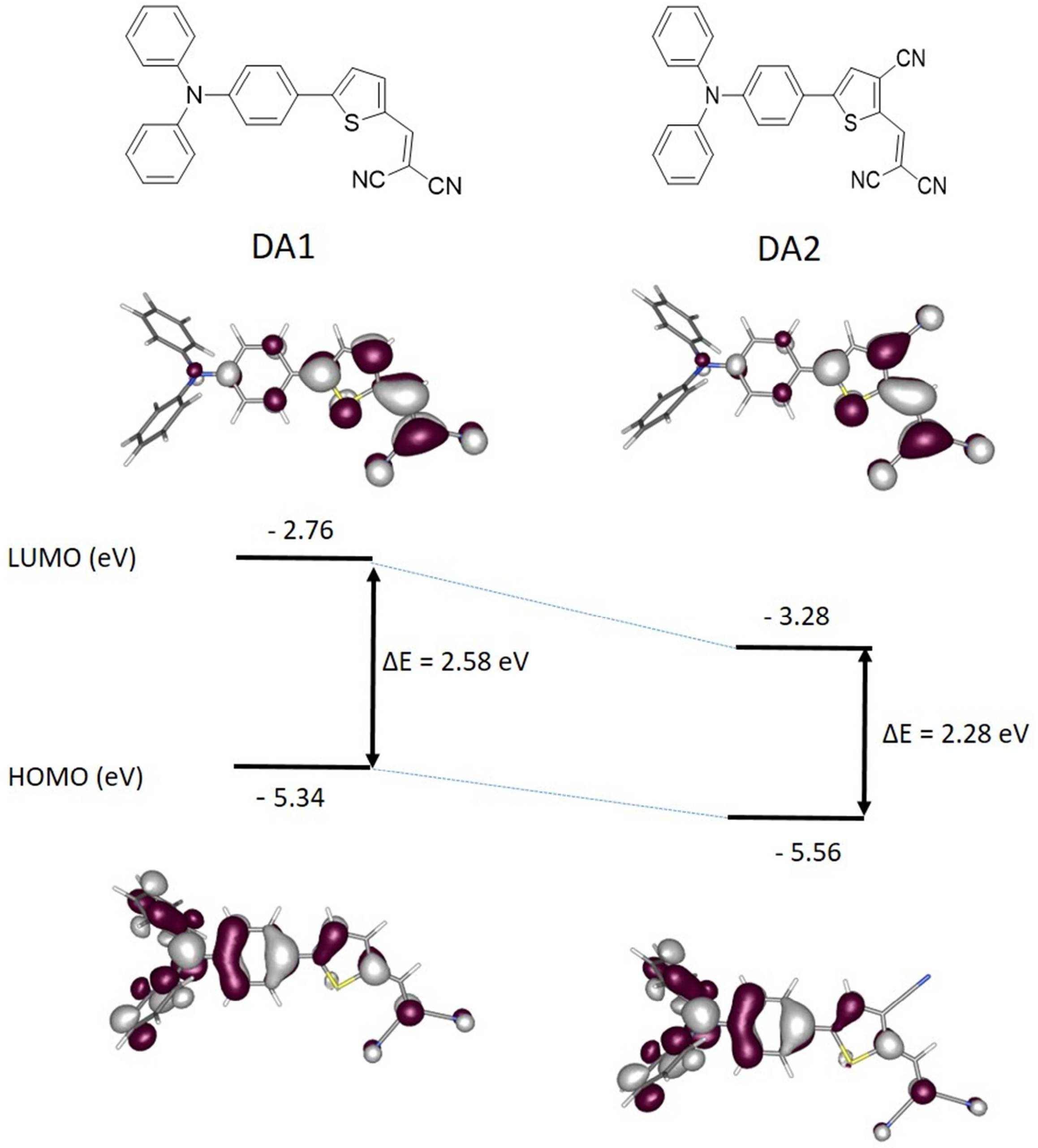

Figure 3: Calculated HOMOs and LUMOs and schematic representation of the energy levels for **DA1** and **DA2**.

The UV-vis absorption spectra of **DA1** and **DA2** have been recorded in methylene chloride and from thin film spun casted on glass sheets (Figure 4 and Table 2). Both compounds exhibit an intense absorption band in the 400 – 700 nm region assigned to an internal charge transfer (ICT transition). In solution, **DA1** presents a maximum wavelength λ_{max} at 500 nm with a molecular absorption coefficient ε_{DA1} of 34232 L.mol^{-1}cm^{-1}. It turns out that the insertion of the cyano group on the thiophene connector **(DA2)** both leads to an increase of ε and a red shift of the absorption band of ca 50 nm. In solid state, the absorption bands of titled compounds are broadened and red shifted with maxima of the absorption bands around 521 and 573 nm corresponding to band gaps, calculated from the foot edge of the absorption bands, of ca 1.95 and 1.77 eV for **DA1** and **DA2** respectively. This difference of ca 0.18 eV, due to the electro-deficient cyano group grafted on the thiophene, is in good agreement with the theoretical calculation.

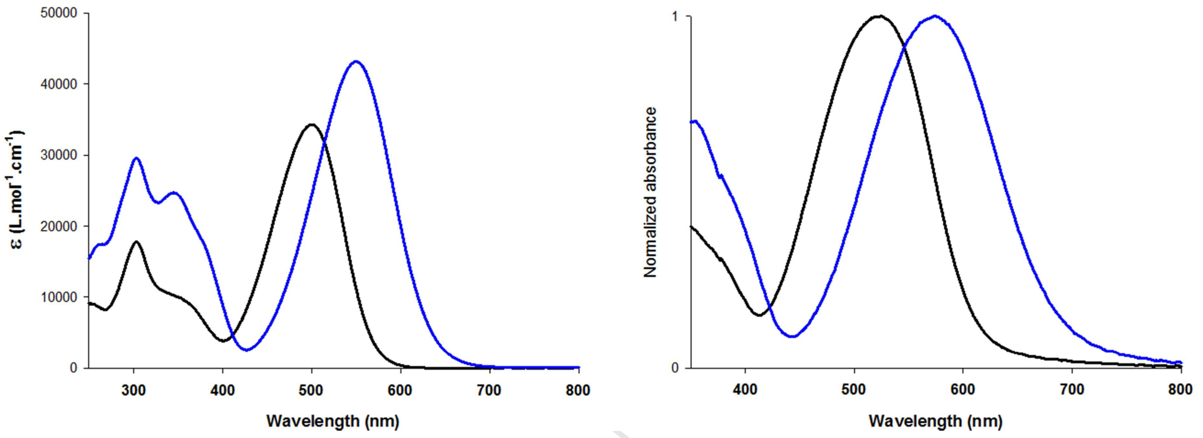

Figure 4 : Left) UV/Vis absorption spectra in solution (10^{-5} M in CH_2Cl_2) of **DA1** (black) and **DA2** (blue; Right) Normalized absorption spectra of films of **DA1** (black) and **DA2** (blue).

Cyclic voltammograms (CVs) of **DA1** and **DA2,** recorded in dichloromethane using Bu_4NPF_6 as supporting electrolyte, show very close reversible oxidation peaks at 1.00 and 1.07 V respectively (Figure 5 and Table 2). In contrast, the irreversible reduction peak of **DA2** is positively shifted by 380 mV compared to **DA1**. Considering the onsets of the oxidation and reduction waves, both materials display very close experimental HOMOs (–5.89 eV and -5.90 eV for **DA1** and **DA2** respectively), whereas the LUMOs are well differenced (-3.95eV vs -4.35 eV for **DA1** and **DA2** respectively). Once again, these results agree with the theoretical calculations since the insertion of the cyano group mainly contributes in stabilizing the LUMO level of **DA2**.

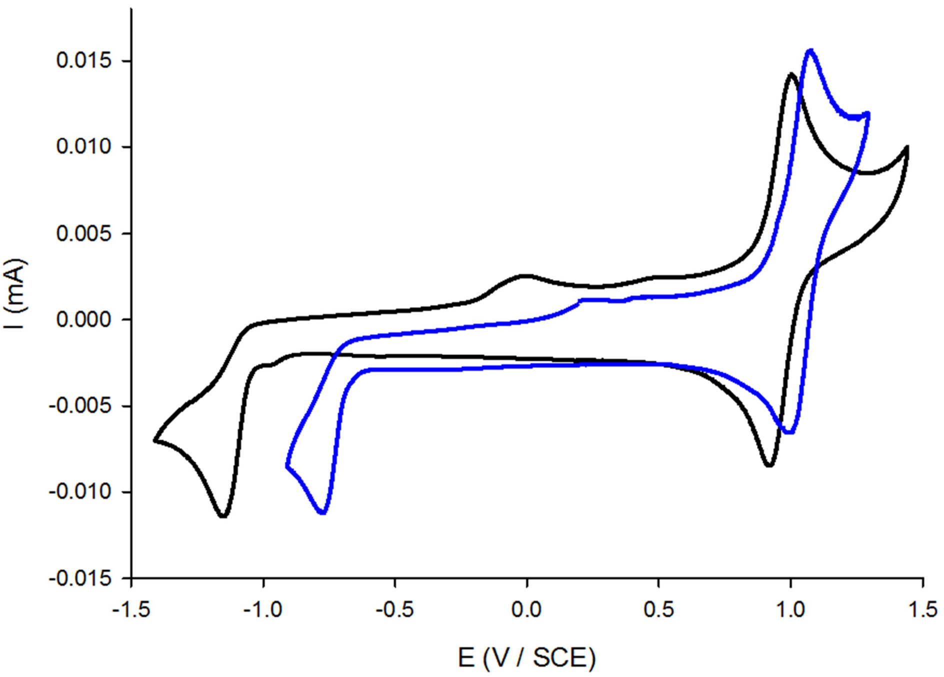

Figure 5: CVs of **DA1** (black) and **DA2** (blue) 10^{-3} M in 0.1 M Bu_4NPF_6 in CH_2Cl_2, v = 100 mV.s^{-1}

Table 2: Optical and electrochemical data of **DA1** and **DA2**

Compd.	λ_{max} [a] nm	ε_{max} [a] $Lmol^{-1}cm^{-1}$	E_g [b] eV	E_{ox} [c] V	E_{red} [c] V	E_{HOMO} [d] V	E_{LUMO} [d] V	ΔE_{elec} eV
DA1	500	34232	1.94	1.00	-1.15	-5.89	-3.95	1.94
DA2	550	43217	1.77	1.07	-0.77	-5.90	-4.35	1.55

[a] 10^{-5} M in CH_2Cl_2. [b] From the foot edge bands absorption of films spun-cast on glass. [c] 10^{-3}M in 0.1 M Bu_4NPF_6–CH_2Cl_2, 100 mV.s^{-1}, Pt working electrode, ref. SCE. [d] Using an offset of -4.99 eV vs. vacuum level for SCE.[34]

The potential of **DA2** as donor material has been evaluated and compared to **DA1** in basic bilayer planar heterojunction solar cells (PHJ). The cells were prepared by spin-casting a chloroform solution of donor onto indium tin oxide (ITO) precoated with poly(3,4-ethylenedioxythiophene):poly(styrenesulfonate) (PEDOT/PSS). Then a 30 nm layer of C_{60} was deposited by thermal evaporation under vacuum, followed by the deposition of an 80 nm aluminium electrode (27 mm² of active area). Annealing tests of the films have been performed at different temperatures. Results are gathered in Table 3 and the current voltage of the cells are presented in Figure S5 in supplementary materials.

Solar cells fabricated with the reference compound **DA1** are characterized by a moderate average open-circuit voltage (V_{OC}) of ca 0.72 V, a fill factor (FF) of 0.36 and a relatively high short-circuit current density (J_{SC}) for a bilayer cells of 6.91 mA.cm^{-2}, resulting in an average PCE of 2.26 % (best of 2.46 %). In comparison, compound **DA2** based OSCs are slightly less efficient with a PCE close to 2% due to a decrease of both the V_{OC} (0.66 V) and the FF (0.31). However, it is noteworthy that high J_{SC} up to 7.5 mA.cm^{-2}, were reached. In parallel, measurements of the hole mobility (μ^h), using the space charge limited current method using the Mott-Gurney law, show very close results μ^h of *ca* 1.1x10^{-5} and 0.9x10^{-5} cm^{2}V^{-1}s^{-1} for **DA1** and **DA2** respectively (Figure S6 in SI). To gain further insights, comparison of the external quantum efficiency (EQE) spectra were performed on best devices (Figure 6). The latter, in consistency with the UV-visible spectra and the Jsc parameters, reveal that grafting the cyano on the thiophene connector results in a significant extension of the contribution of the donor in the long wavelengths region. From these results, it turns out that blending these two complementary donors should increase the charge carrier generation.[35-39]

Indeed, this efficient strategy has already been demonstrated in ternary blends for bulk heterojunction solar cells where two donors were successfully mixed with the fullerene derivative.[40-42]

Thus, the similar crystallinity, suggested by the X-ray structures, the good complementarity in absorption coupled to comparable hole mobility, suggest that the two donors **DA1** and **DA2** should be compatible and would even team up to improve the overall efficiency. In this context, bilayer solar cells based on an equimolar blend of **DA1** and **DA2** for the donor materials and C_{60} for the acceptors materials were prepared (Figure S5 in supplementary materials). It turns out that even if the FF slightly decreased the V_{OC} overtook +0.84 V and the

Jsc parameter rose to 8.4 mA.cm^{-2} achieving a maximum PCE of ca 3.1%. Although we have no rational explanation for the increasing of the V_{OC} for the blend of **DA1** and **DA2**, that present similar HOMO level, it is worth noting that the origin of the theoretical V_{OC} of organic photovoltaic devices has yet to be determined. Recent works demonstrated the influence on the V_{OC} values of the donor – acceptor interactions at the interface between small donor molecules and acceptors.[43, 44] The EQE spectrum for the blend confirms a synergic contribution of the absorption of the two compounds in the 650 – 400 nm region. This result confirms the compatibility of the molecules through aggregation and crystallization to give well organized active layers favourable to increase the J_{SC} value.

Table 3. Photovoltaic characteristics of PHJ cells based on donor **DA1** and **DA2** and under 1.5-simulated solar illumination at 90 mW cm^{-2} after 5 min annealing

Compound	$T_{annealed}$ (°C)	Average V_{OC} (V)	Average Jsc (mA cm^{-2})	Average FF	Average PCE (%)	Best PCE (%)
DA1	120	0.72	6.91	0.36	2.26	2.46
DA2	140	0.66	7.52	0.31	1.91	1.96
DA1 + **DA2**	120	0.84	8.38	0.30	2.66	3.06

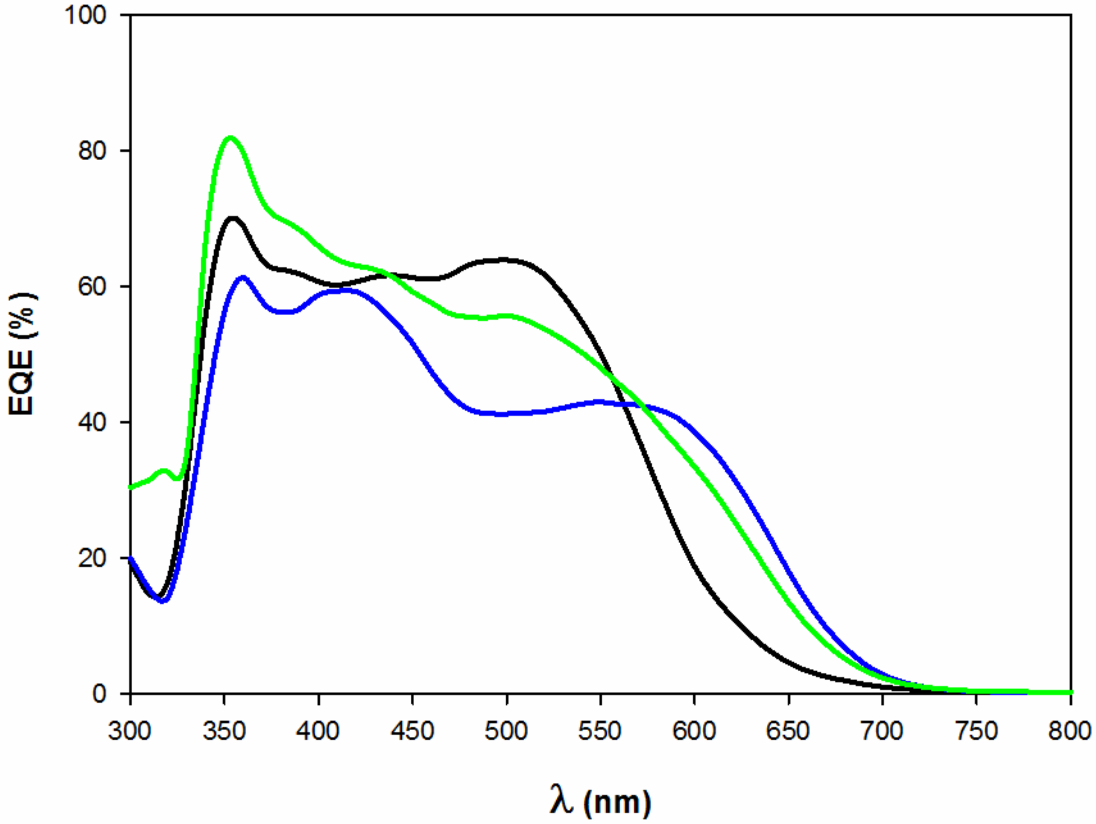

Figure 6. External quantum efficiency (EQE) of the cells produced with donors **DA1** (black), **DA2** (blue) and a blend of **DA1** and **DA2** (green)

Conclusion

In summary, we have prepared two analogous donors whose syntheses have been performed by the greenest routes as possible, i.e., through direct arylation using C-H bond activation and Knoevenagel condensation without any solvent. We have examined the effects of a small structural modification on the electronic properties and on the photovoltaic performances of basic bilayer solar cells. An efficient improvement of the performance of the cells was demonstrated when active layers were built with blend of donors. We demonstrate that the minor molecular change for the donor materials allowed a sufficient variation of the electronic properties without strong modification in the supramolecular organizations in the solid state. Thus, the advantage of the binary active layer for enhancing the harvesting of photons is related to the synergistic effects of similar self-assembly properties, hole mobility and complementary absorption of the titled materials.

References

[1] A.K. Pandey, V.V. Tyagi, J.A.L. Selvaraj, N.A. Rahim, S.K. Tyagi, Renew. Sustain. Energy Rev. 53 (2016) 859-884.
[2] K.A. Mazzio, C.K. Luscombe, Chem. Soc. Rev. 44 (2015) 78-90.
[3] L. Lu, T. Zheng, Q. Wu, A.M. Schneider, D. Zhao, L. Yu, Chem. Rev. 115 (2015) 12666-12731.
[4] L. Dou, J. You, Z. Hong, Z. Xu, G. Li, R.A. Street, Y. Yang, Adv. Mater. 25 (2013) 6642-6671.
[5] X. Liu, H. Chen, S. Tan, Renew. Sustain. Energy Rev. 52 (2015) 1527-1538.
[6] U. Mehmood, A. Al-Ahmed, I.A. Hussein, Renew. Sustain. Energy Rev. 57 (2016) 550-561.
[7] V. Malytskyi, J.-J. Simon, L. Patrone, J.-M. Raimundo, RSC Adv. 5 (2015) 354-397.
[8] A. Mishra, P. Bäuerle, Angew. Chem. Int. Ed. 51 (2012) 2020-2067.
[9] R. Po, A. Bernardi, A. Calabrese, C. Carbonera, G. Corso, A. Pellegrino, Energy Environ. Sci. 7 (2014) 925-943.
[10] D.J. Burke, D.J. Lipomi, Energy Environ. Sci. 6 (2013) 2053-2066.
[11] G. Marzano, C.V. Ciasca, F. Babudri, G. Bianchi, A. Pellegrino, R. Po, G.M. Farinola, Eur. J. Org. Chem. 2014 (2014) 6583-6614.
[12] T.P. Osedach, T.L. Andrew, V. Bulovic, Energy Environ. Sci. 6 (2013) 711-718.
[13] J. Roncali, P. Leriche, P. Blanchard, Adv. Mater. 26 (2014) 3821-3838.
[14] H. Bürckstümmer, E.V. Tulyakova, M. Deppisch, M.R. Lenze, N.M. Kronenberg, M. Gsänger, M. Stolte, K. Meerholz, F. Würthner, Angew. Chem. Int. Ed. 50 (2011) 11628-11632.
[15] L.-Y. Lin, Y.-H. Chen, Z.-Y. Huang, H.-W. Lin, S.-H. Chou, F. Lin, C.-W. Chen, Y.-H. Liu, K.-T. Wong, J. Am. Chem. Soc. 133 (2011) 15822-15825.
[16] Y.-H. Chen, L.-Y. Lin, C.-W. Lu, F. Lin, Z.-Y. Huang, H.-W. Lin, P.-H. Wang, Y.-H. Liu, K.-T. Wong, J. Wen, D.J. Miller, S.B. Darling, J. Am. Chem. Soc. 134 (2012) 13616-13623.
[17] A. Leliege, C.H. Le Regent, M. Allain, P. Blanchard, J. Roncali, Chem. Commun. 48 (2012) 8907-8909.
[18] A. Leliège, J. Grolleau, M. Allain, P. Blanchard, D. Demeter, T. Rousseau, J. Roncali, Chem. Eur. J. 19 (2013) 9948-9960.
[19] Y. Jiang, C. Cabanetos, M. Allain, P. Liu, J. Roncali, J. Mater. Chem. C 3 (2015) 5145-5151.
[20] V. Jeux, D. Demeter, P. Leriche, J. Roncali, RSC Adv. 3 (2013) 5811-5814.
[21] A. Labrunie, Y. Jiang, F. Baert, A. Leliege, J. Roncali, C. Cabanetos, P. Blanchard, RSC Adv. 5 (2015) 102550-102554.
[22] F. Baert, C. Cabanetos, M. Allain, V. Silvestre, P. Leriche, P. Blanchard, Org. Letters 18 (2016) 1582-1585.
[23] C. Moussallem, F. Gohier, C. Mallet, M. Allain, P. Frère, Tetrahedron 68 (2012) 8617-8621.
[24] C. Moussalem, O. Segut, F. Gohier, M. Allain, P. Frère, ACS Sustainable Chem. Eng. 2 (2014) 1043-1048.
[25] C. Sissa, V. Parthasarathy, D. Drouin-Kucma, M.H.V. Werts, M. Blanchard-Desce, F. Terenziani, Phys. Chem. Chem. Phys. 12 (2010) 11715-11727.
[26] Z.B. Wang, M.G. Helander, M.T. Greiner, J. Qiu, Z.H. Lu, J. Appl. Phys. 107 (2010) 034506.
[27] D.J. Schipper, K. Fagnou, Chem. Mater. 23 (2011) 1594-1600.
[28] D. Demeter, S. Mohamed, A. Diac, I. Grosu, J. Roncali, ChemSusChem 7 (2014) 1046-1050.
[29] A. Diac, D. Demeter, M. Allain, I. Grosu, J. Roncali, Chem. Eur. J. 21 (2015) 1598-1608.

[30] G. Kaupp, M. Reza Naimi-Jamal, J. Schmeyers, Tetrahedron 59 (2003) 3753-3760.
[31] B. Rodríguez, A. Bruckmann, T. Rantanen, C. Bolm, Adv. Synth. Catal. 349 (2007) 2213-2233.
[32] R.A. Sheldon, Chem. Commun. 29 (2008) 3352-3365.
[33] S. Fuse, S. Sugiyama, M.M. Maitani, Y. Wada, Y. Ogomi, S. Hayase, R. Katoh, T. Kaiho, T. Takahashi, Chem. Eur. J. 20 (2014) 10685-10694.
[34] C.M. Cardona, W. Li, A.E. Kaifer, D. Stockdale, G.C. Bazan, Adv. Mater. 23 (2011) 2367-2371.
[35] L. Yang, H. Zhou, S.C. Price, W. You, J. Am. Chem. Soc. 134 (2012) 5432-5435.
[36] B.M. Savoie, S. Dunaisky, T.J. Marks, M.A. Ratner, Adv. Energy Mater. 5 (2015) 1400891.
[37] N. Felekidis, E. Wang, M. Kemerink, Energy Environ. Sci. 9 (2016) 257-266.
[38] T. Ameri, P. Khoram, J. Min, C.J. Brabec, Adv. Mater. 25 (2013) 4245-4266.
[39] Y.-C. Chen, C.-Y. Hsu, R.Y.-Y. Lin, K.-C. Ho, J.T. Lin, ChemSusChem 6 (2013) 20-35.
[40] T. Rousseau, A. Cravino, T. Bura, G. Ulrich, R. Ziessel, J. Roncali, J. Mater. Chem. 19 (2009) 2298-2300.
[41] J.A. Mikroyannidis, D.V. Tsagkournos, S.S. Sharma, A. Kumar, Y.K. Vijay, G.D. Sharma, Sol. Energy Mater. Sol. Cells 94 (2010) 2318-2327.
[42] M.E. Farahat, D. Patra, C.-H. Lee, C.-W. Chu, ACS Appl. Mater. Interfaces 7 (2015) 22542-22550.
[43] S.-W. Liu, W.-C. Su, C.-C. Lee, C.-F. Lin, C.-W. Cheng, C.-C. Chou, J.-H. Lee, C.-T. Chen, Sol. Energy Mater. Sol. Cells 109 (2013) 280-287.
[44] Y. Zou, R.J. Holmes, ACS Appl. Mater. Interfaces 7 (2015) 18306-18311.

Graphical abstract